博士論文

Roles of ACF7, a large linker protein interacting with both microtubules and filamentous actin, in dendrite morphogenesis and postsynaptic maturation

（樹状突起の形態形成及びシナプス後部制御における細胞骨格相互結合タンパク質 ACF7 の機能解析）

柏木　有太郎

博士論文

Roles of ACF7, a large linker protein interacting with both microtubules and filamentous actin, in dendrite morphogenesis and postsynaptic maturation

（樹状突起の形態形成及びシナプス後部制御における細胞骨格相互結合タンパク質 ACF7 の機能解析）

所属：東京大学大学院　医学系研究科　分子細胞生物学専攻

指導教員：岡部 繁男 教授

申請者名：柏木　有太郎

Table of contents

1. Abstract 2

2. Introduction 3

3. Materials & Methods 8

4. Results 16

5. Discussion 27

6. Acknowledgements 33

7. Reference 34

8. Figure Legends 42

9. Figures 50

Abstract

The morphological changes of neurons are essential to establish proper neuronal connection during development. Cellular morphogenesis is based on changes of the underlying two major cytoskeletons, microtubules (MTs) and filamentous actin (F-actin). Although MTs and F-actin have distinct roles, the spatial organization between MTs and F-actin are tightly coordinated during neuronal development. Accumulating evidence suggests that MT-actin interaction is mediated by cytoskeleton crosslinking proteins. ACF7/MACF1 is a member of spectraplakin family protein and able to bind both MTs and F-actin directly. Although ACF7 is expressed in the central nervous systems, the physiological significance of ACF7 in neurons has remained unknown.

Here, by using hippocampal dissociate culture and manipulation of ACF7 content at two different developmental stages, I report that ACF7 is essential for dendrite outgrowth and postsynaptic maturation. During early developmental stages, ACF7 accumulated the region where MTs and F-actin are in close contact, such as growth cones and enhanced dendrite outgrowth. In a later developmental stage, ACF7 clustered in a subset of dendritic spines and enhanced structural maturation of individual spines locally. These results may indicate that ACF7 maintains MT-actin interaction even in a subset of spines and contributes to proper excitatory synapse development.

Introduction

After birth and migration within specific cortical layers or nuclei, neurons break their previous symmetry and establish two distinct cellular structures termed axon and dendrite. The contact sites between presynaptic axons and postsynaptic dendrites start to differentiate into synapses. After establishment of initial synaptic connections, neuronal circuits are refined by the formation and elimination of synapses. Appropriate regulation of neuronal morphology during development is essential for the establishment of proper functional circuits in the brain[1–6].

Coordination of microtubule-actin interactions in neuronal morphogenesis

Morphogenesis of neurons is greatly influenced by the dynamic reorganization of microtubules (MTs) and filamentous actin (F-actin). In the early stage of neuronal development, the interaction between MTs and F-actin is essential for neuritegenesis[7,8], neurite outgrowth[9] and axon branching[10]. Especially, MT-actin interaction in the growth cone, a specialized terminal structures at the tip of developing neuronal processes, has been investigated well. A large bundle of MTs are recognized in the central domain of growth cone and a sub-population of the dynamic MT plus ends penetrates into the actin rich peripheral domain[11,12]. The dynamics of these two cytoskeletal components affect the shape of growth

cone and guide its movement to establish proper wiring of the brain[3,11–14]. MT-actin interaction within growth cones can potentially be mediated by either pairs of protein that contain single MT- or actin-binding domains, or by large protein molecules that can cross-link between MT and F-actin[15–17]. Although it has been emphasized that the interaction between MT-actin is essential for neurite morphogenesis during early neuronal development, recent findings start to shed light on roles of MT-actin interactions in mature neuron[18,19].

Crosstalk between MTs and F-actin in excitatory synapses

In the pyramidal neurons, most excitatory synapses are formed onto dendritic spines that protrude from main shafts of dendrites[18,20]. The cytoskeletal distribution in dendrites and dendritic spines seems to be distinct[21]. Actin filaments are closely associated with both spine plasma membrane and the cytoplasmic surface of the PSDs [22,23]. By contrast, bundled MTs are mainly recognized within dendritic shafts and a sub-population of the dynamic MT plus ends penetrates into dendritic spines[24–26].

It is widely accepted that the actin cytoskeleton has prominent roles in determining dendritic spine morphology and in anchoring postsynaptic proteins[19,20,27,28]. However, MTs are also essential for development and function of synapses. The MT-dependent transport system that delivers a wide variety of trafficking cargoes and organelles from soma to synapses should be coordinated with the actin-dependent system[29–32]. Furthermore, recent

studies suggest that dynamic MTs penetrating into spines can modulate actin dynamics within spines[33]. Dynamic MTs may contribute to critical events in synapse development, such as spine structural maturation and PSD formation[34–36]. It has been emphasized that the crosstalk between MTs and F-actin are tightly regulated during synapse development and synaptic function. Although molecular mechanisms underlying coordination of the MTs and F-actin in dendrites and spines are largely unknown, accumulating evidence suggests the presence of MT-actin crosslinking proteins even in mature neuron.

Interaction between MTs and F-actin via spectraplakin family proteins

Spectraplakins are multifunctional giant (>500 kDa) cytoskeletal proteins which have both MT and F-actin binding domains[16,37–39]. Spectraplakins have an F-actin binding motif in their N-terminal domain. Within the C-terminal domain of spectraplakin, there are two MT binding motif; a GAR domain of spectraplakin associates with MTs and a CTD domain can interact with EB1, a protein which binds to the growing ends of MTs[40–42]. Two discrete cytoskeletal interaction domains are physically separated by a large number of spectrin repeats which are thought to provide molecular flexibility[43–45].

Spectraplakins are broadly expressed and conserved among species. Null mutation in spectraplakins result in a wide variety of tissue and cellular defects including aberration of

MT-actin organization and cell-cell adhesion[17,37]. Of the mammalian spectraplakins, ACF7/MACF1 (actin crosslinking family 7/ microtubule and actin crosslinking factor 1) is present early in embryonic development. ACF7 is highly expressed in neuronal tissues and the foregut of embryonic day 8.5; Early developmental lethality of ACF7 KO mice prevented analysis of ACF7-null phenotype in the mature nervous system[46].

To overcome this problem, nervous tissue specific ACF7 KO mice were established using Cre/loxP technology[47]. However, these ACF7 nestin-cKO mice die within 24-36 h after birth of apparent respiratory distress. ACF7 nestin-cKO brain displays multiple developmental defects including a disorganized cerebral cortex, heterotopia of the hippocampal pyramidal layer, and aplasia of the corpus callosum and hippocampal commissures[47].

Although ACF7function may be important in potential development of differentiated neuron and their functional connectivity via synapses, roles of ACF7 in differentiated neurons have not yet been investigated. Recent proteomic analyses of biochemically purified PSD fractions identified ACF7 as a candidate PSD component[48,49], suggesting possible involvement of ACF7 in synaptic functions.

To explore the function of ACF7 in neurons, I manipulated ACF7 content in hippocampal dissociated culture. An advantage of this approach is that it allows us to determine the ACF7 phenotype in neurons at both early and later stages of development. This is not possible in ACF7 knockout mice due to embryonic and postnatal lethality[46,47,50]. Here, I report that ACF7 is essential for two developmental stages in neurons. In an early stage of development, ACF7 accumulates at the region where MTs and F-actin are in close contact, such as growth cones. Knock-down of endogenous ACF7 severely suppresses dendrite outgrowth and its crosslinking function is essential for enhancement of dendrite outgrowth.

In mature neurons, the synaptic clusters of ACF7 were detected within a subset of spines. Overexpression of ACF7 induced local maturation of individual spines containing ACF7 clusters, and down-regulation of ACF7 inhibited excitatory synapse development. These results may indicate that ACF7 maintains proper MT-actin interaction at a subset of spines. I hypothesize that ACF7 regulates dynamics of MTs penetrating into spines and subsequently enhances postsynaptic growth.

Materials & Methods

Mice

All animal experiments performed in this study were conducted in accordance with guidelines established by the animal welfare ethics committee at the University of Tokyo. ACF7 floxed mutant mice were obtained from the Jackson Laboratory.

Generation of anti-ACF7 antibody

For generating anti-ACF7 polyclonal antibody, GST fusion proteins were engineered to contain the amino acid sequence 1,000 to 1,208 of mouse ACF7 (Gene ID: 11426), corresponding to the plakin domain. The DNA fragment was inserted into the pGEX-4T1 vector (GE healthcare). Proteins were expressed in *E.coli* strain BL21 and purified using binding to GST-conjugated Sepharose beads. The GST tags were cut out after purification. The recombinant proteins were immunized into New Zealand White rabbits. The resulting anti serum was further purified by affinity chromatography.

Construction of expression plasmids

To isolate cDNAs of mouse ACF7 (Gene ID: 11426), the total RNA was extracted from mouse C57BL/6 brain by using RNeasy mini (QIAGEN). RT-PCR was performed using the SuperScript Ⅱ reverse transcriptase (Life Technologies) and cDNAs were amplified using KOD+ polymerase (TAKARA). All procedures were performed according to the manufacture's protocols. The PCR products were subcloned into pGEM-T vector (Promega) for sequencing. The sequence of this cDNA is consistent with ACF7 neuronal isoform2 (NP_001186066) which contains both CH1 and CH2 domain. The ACF7 cDNA was inserted into pEGFP-N2 vector (Clontech) to generate ACF7-GFP. DNA fragments corresponding to actin binding domain (amino acids 1-432 of ACF7) or MT binding domain (amino acids 5054-5430 of ACF7) were also inserted into pEGFP-N2 vector to generate ACF7(NT)-GFP or ACF7(CT)-GFP. For neuronal expression of exogenous tagged proteins, the DNA fragments containing coding regions of the proteins were inserted into the multiple cloning site of a vector with the upstream β-actin promoter sequences. pAct-LacZ and an adenovirus for the expression of Cre recombinase were described previously[51,52].

RNA interference

As small interfering RNA (siRNA) sequence targeting ACF7 expression in cells,

nucleotides 373-393 (amino acids 68-74; gccgtggtccgagtcgctgat) of ACF7 were selected[46]. The oligonucleotides were subcloned into the pSilencer siRNA expression vector (Invitrogen). Stealth™ RNAi Negative Control Duplexes (Invitrogen) were used as control shRNA. The sequence of resistant form of ACF7 was designed by introducing triple point mutations into the original sequences using QuickChange Site-Directed Mutagenesis Kit (Stratagene) .

Biochemical purification of PSDs

PSD fractions were prepared from rat forebrains essentially as previously described[53,54]. Young adult mice were rapidly decapitated after anesthetized deeply, brains were removed, and homogenized in ice-cold HEPES-buffered sucrose (0.32 M sucrose, 4 mM HEPES, pH 7.4) containing a protease inhibitor cocktail (Sigma-Aldrich) with Teflon homogenizer. Homogenized brain extract was spun at 1,000 ×*g* for 10 min to remove the nuclear fraction. Supernatant (S1) was centrifuged at 10,000 × *g* for 15 min to yield the crude synaptosomal fraction (P2). P2 was resuspended in HEPES-buffered sucrose and then respun at 10,000 × *g* for another 15 min. The resulting pellet was resuspended in HEPES buffer (4 mM HEPES, pH 7.4) with Teflon homogenizer, and mixed constantly for 30 min at 4^{o}C. After centrifugation of the lysate at 25,000 × *g* for 20 min, the supernatant was saved as crude synaptic vesicle fraction (S3), and the pellet (P3) was responded in HEPES-buffered 0.32 M sucrose. The P3

suspension was then carefully loaded onto a discontinuous sucrose gradient (0.8 M/1.0 M/1.2 M sucrose solution in 4 mM HEPES, pH 7.4), and centrifuged at 150,000 × *g* for 2 h in a SW-40 rotor (Beckman). Synaptic plasma membranes (SPM) were recovered in the layer between 1.0 M and 1.2 M sucrose and resuspended in HEPES buffer to the final concentration of 0.32 M sucrose. Sample was spun at 150,000 × *g* for 30 min and the resulting pellet was resuspended in HEPES -EDTA buffer (50 mM HEPES and 2 mM EDTA, pH 7.4). Further purification of PSDs was performed adding concentrated stock solution of Triton X-100 to the final concentration of 0.5%, by followed gentle agitation at 4^{o}C for 15 min, and subsequent centrifugation at 32,000 × *g* for 20 min in a TLA 55 rotor (Beckman). The resulting pellet was resuspended in HEPES-EDTA buffer (PSD-1T fraction). Next round of wash with Triton X-100 and sedimentation of PSDs with a stronger centrifugation condition (at 200,000 × *g* for 20 min in a TLA 100 rotor) was performed to obtain PSD-2T fraction. To obtain synaptic vesicle (SV) fraction, saved crude synaptic vesicle fraction was centrifuged at 165,000 × *g* for 2 h.

Western blotting

Samples were separated by 5-15 % SDS-PAGE and transferred onto nitrocellulose membranes (Millipore). The membranes were blocked with 5 % skim milk in TBS for 1 hour

at room temperature and probed with antibodies overnight at 4 ^{o}C. The primary antibodies were rabbit polyclonal anti-ACF7 antibody, mouse monoclonal anti-α-tubulin antibody (Sigma-Aldrich), mouse monoclonal anti-PSD-95 antibody (Neuromab), and rabbit polyclonal anti-synaptophysin (Boehringer Mannheim Biochemica). Secondary antibodies were peroxidase labeled goat antibodies against mouse or rabbit IgG (Amersham).

Cultures

Mouse embryonic fibroblasts (MEFs) were isolated from E13.5 ACF7$^{flox/flox}$ embryos. MEFs, COS-7 cells and 3T3 cells were cultured in DMEM media (Life Technologies) containing 10 % FCS, 5 Units/ml Penicillin, 5 μ g/ml streptomycin and GlutaMAX supplement (GIBCO). Cells were transfected with expression plasmids using Xtreme GENE HP DNA Transfection Reagent (Roche).

Dissociated hippocampal neurons from 16-day-old embryonic mice were plated onto glass coverslips coated with poly-L-lysine and maintained in Minimum Essential Medium (MEM) with B18 supplement and 5% FCS. Two days after plating, 5 μM ara-C was added to prevent glial cell proliferation. Hippocampal neurons were transfected by calcium phosphate method. Live cells were replaced into the prewarmed Tyrode's solution (119 mM NaCl, 2.5 mM KCl, 2 mM Ca^{2+}, 2 mM Mg^{2+}, 25 mM HEPES, pH 7.4 and 30 mM glucose) for 30 min before the

treatment. Concentrated stocks of latrunculin A (Molecular Probes) and vincristine (Sigma-Aldrich) were added to Tyrode's solution and the final concentration of latrunculin A and vincristine was 5 μM. After 5 hr treatment at 37 ℃, cells were immediately examined.

Immunostaining of dissociated neurons and brain sections

In most experiments, cells were fixed in 2 % paraformaldehyde in PBS for 25 min at room temperature and treated with 0.2 % Triton X-100 in PBS for 25 min. In some experiments, methanol solution were used to fix cells for 10 min at -20 ℃. Culture preparations were blocked with 5 % NGS and reacted with the first antibodies and secondary antibodies. The primary antibodies were rabbit polyclonal anti-ACF7, anti-β-galactosidase (Cappel), anti-GFP, anti-HA (MBL) : mouse monoclonal anti-α-tubulin, anti-MAP2 (Sigma-Aldrich), anti-PSD-95 (Thermo Scientific Pierce Antibodies), anti-EB1 (BD Transduction Laboratories) anti-β-galactosidase (Promega) : Secondary antibodies: Alexa488 conjugated anti-mouse/rabbit IgG: Invitrogen, or Cy3 conjugated anti-mouse/rabbit IgG (Jackson ImmunoResearch) or Alexa633 conjugated anti-mouse/rabbit IgG (Invitrogen), rhodamine-conjugated phalloidin (Molecular Probes).

Image analysis

Images were obtained were using a Fluoview confocal laser-scanning microscope (Olympus, Tokyo, Japan) with 20× dry objective lens or 60× oil immersion lens. Image analyses and quantification were performed by using Metamorph software (Molecular Devices) or ImageJ software (NIH). Multiple images with different focal planes were projected into a single image using a maximum-brightness operation.

For the measurement of total dendrite length, all dendrites of individual neurons were traced manually, and the number of pixels were calculated automatically. To perform sholl analysis, dendrite morphology was first traced by Neuron J plugin. The data were quantified by Sholl Analysis plugin for ImageJ, examining each 20 μm segment of the dendritic tree. To quantify spine morphology, one to three segments of secondary dendrites were collected from each neurons. Length of all protrusions were determined by tracing the protrusion manually. To quantify spine volume, GFP or Alexa633 fluorescence within each dendritic spine were quantified. To determine intensity of PSD-95, fluorescent puncta were extracted automatically with an identical setting of thresholding and the thresholded images were measured by integrated morphometry analysis using Metamorph software . Individual measurements were averaged per neuron. The resulting data were shown as mean±SEM.

Stastical analyses

Stastical analysis was performed GraphPad Prism 6 (GraphPad Software). Data were analyzed by Student's *t*-tests and ANOVA followed by Tukey–Kramer *post hoc* multiple comparison tests.

Results

Expression profile of ACF7 protein in the postnatal developmental brain

Previous gene-targeting studies of ACF7 utilized tissue specific deletion of floxed ACF7 gene by nestin-Cre transgene. Nervous system-specific deletion of ACF7 in the embryonic stage resulted in perinatal lethality with respiratory failure and disorganization of multiple brain structures including the cerebral cortex and the hippocampus[47]. Early lethality and brain malformation precluded further analyses of postnatal functions of ACF7 in fully differentiated neuron in these conditional knockout mice. To test if ACF7 plays a major role in differentiated neuron in the postnatal CNS, I first examined the pattern of ACF7 expression in multiple brain regions, by using an antibody designed to recognize the plakin domain of this molecule. The amino acid sequence of the antigen shares low sequence homology with another member of spectraplakin family present in the postnatal brain, Bpag1/dystonin [46], therefore the antibody is likely to be specific to ACF7.

Western blotting of the extract prepared from the cortex, cerebellum, and hippocampus at postnatal days 7, 14, 21, and 28 revealed a single immunoreactive band with its molecular weight larger than 200 kDa. Although the precise molecular weight of this band was difficult to estimate, I reasoned that this single immunoreactive band corresponds to isoform of ACF7

containing both N-terminal actin binding domain and C-terminal MT binding domain, with its molecular weight of 600 kDa from the following reason. First, the anti-ACF7 immunoreactive band was eliminated after expression of Cre recombinase in MEFs derived from ACF7$^{flox/flox}$ mice. Second, the size of anti-ACF7 immunoreactive band corresponded with anti-GFP immunoreactive band in proteins extracts prepared from ACF7-GFP expressing cells.

In all three brain regions I examined, ACF7 expression was highest at postnatal day 8. Although ACF7 expression decreased gradually in the postnatal development, protein expression is still maintained at postnatal day 28 (Figure 2A), indicating possible roles of ACF7 in maturation of differentiated neurons in the postnatal brain. To see if the pattern of ACF7 expression in cultured neurons follows similar pattern, I examined the level of ACF7 expression in proteins extracts prepared from culture hippocampal neurons maintained in vitro for 7, 14, 21 days (Figure 2B). The peak of ACF7 was at 14 days in vitro. Because hippocampal neurons were dissociated from the embryonic hippocampi at E16, cultured neurons at 14 days in vitro correspond to in vivo neurons at postnatal day 9. Protein expression patterns both in vivo and in culture neurons indicated the presence of expression peak of ACF7 in the early postnatal period and gradual decline of its expression in the postnatal developmental period.

Presence of ACF7 in growth cones of immature hippocampal neurons

I first focused on the subcellular localization of ACF7 in immature hippocampal neurons. Immunocytochemistry of cultured hippocampal neurons using the anti-ACF7 antibodies revealed enrichment of ACF7 protein at the interphase between MT and F-actin at early developmental stage (Figures 3A and B). Although ACF7 was detected throughout the neuron, strong immunoreactivity was found near the tip of neurites (Figure 3A). Furthermore, ACF7 immunoreactivity was strongest in the transition zone between the central and peripheral domains, and also showed +Tips-like pattern at the peripheral domain in both axonal and dendritic growth cones (Figure 3B). To further confirm ACF7 distribution, I transfected ACF7 tagged with GFP (ACF7-GFP) to hippocampal neurons. ACF7-GFP showed MT like localization pattern along dendritic shafts, and it was also observed in an actin-rich peripheral region of growth cone. ACF7-GFP colocalized with both MTs and F-actin in the growth cone (Figure 3C, arrow).

ACF7 is essential for enhancement of dendritic growth

These localization patterns are consistent with the idea that ACF7 is a MT-actin crosslinking protein and regulates neurite outgrowth[50,55]. To verify the roles of endogenous ACF7 in dendrite morphogenesis, I performed loss-of-function analysis. I used a plasmid

vector-based short hairpin RNAs (shRNAs) to suppress the expression of ACF7. The shRNA plasmids were transfected to hippocampal neurons at 4 DIV together with GFP as a marker to visualize neuronal morphology and examined at 9 DIV. The ACF7 shRNA plasmid expressing neurons showed severe impairment of dendrite branching compared with neurons expressing control shRNA plasmid (Figure 4A).

To quantify the pattern of dendrite complexity, I used Sholl analysis, measuring the number of dendrite intersections at each 20 μm radial segment from the cell soma. In control shRNA plasmid expressing neurons, the number of intersections increases with distance from soma, reaching a peak at ~50 μm, and then start to decrease (Figure 4B). In ACF7 shRNA plasmid expressing neurons, the number of intersections simply decreases and reaches zero about 100 μm from soma. Furthermore, ACF7 shRNA caused a decrease (about ~60 %) in the total length of dendrites (Figure 4C). The dendritic phenotype of ACF7 knock-down was rescued by expression of an RNAi-resistant forms of ACF7, with slightly increase in both number of dendrite intersections and total dendrite length (Figures 4A, B and C). Thus, these data suggest that ACF7 is essential for dendritic morphogenesis.

To clarify the molecular basis for the function of ACF7 in dendrite morphogenesis, I investigated the role of its cytoskeleton binding domains. I constructed full length ACF7, the

actin binding domain and the MT binding domain of ACF7. These protein were fused to GFP and transfected into hippocampal neurons at 4 DIV together with *lacZ*. The morphology of dendrites was visualized by anti-β-galactosidase immunostaining. At 5 days after transfection, the ACF7-GFP expressing neuron showed excess dendrite branching compared with neurons expressing GFP (Figure 4D). By contrast, neurons expressing either the N-terminal actin binding domain of ACF7 (ACF7 (NT)-GFP) or the C-terminal MT binding domain of ACF7 (ACF7 (CT)-GFP) showed severe impairment of dendrite branching. Sholl analysis and measurement of total dendrite length also indicated enhancement of dendrite branching by the overexpression of ACF7 but not its deletion mutants (Figures 4E and F). These results suggest that coordination of MT-actin interaction is essential for enhancement of dendrite outgrowth. Thus, ACF7 is essential for proper dendrite morphogenesis and it acts as a cytoskeletal crosslinker in early neuronal development.

Presence of ACF7 in postsynaptic compartments

The cytoskeletal microdomains seems to be spatially separated in mature neurons[21,56]. Actin filaments are predominately concentrated in both presynaptic terminals and postsynaptic sites, while MTs are mainly restricted within axonal and dendritic shafts[19,21,27]. ACF7 relates to both MTs and F-actin, and its expression continued even in mature brains (Figures 2A and B). Thus, I next focused on the localization and function of ACF7 in mature neurons.

Cultured hippocampal neurons at 3 weeks after plating were stained by using the anti-ACF7 and anti-α-tubulin antibodies, and rhodamine conjugated phalloidin. In mature neurons, ACF7 was also detected throughout the neuron and showed strong immunoreactivity within soma (Figure 5A). ACF7 was distributed along dendrites, and some strong accumulation was present in structures projecting from dendritic shafts (Figure 5B) The ACF7 accumulation showed heterogeneity, and its clustering was frequently colocalized with phalloidin staining. This localization pattern is consistent with the concept that ACF7 interacts with both MTs and F-actin.

ACF7 is a candidate PSD component[48,49]. To clarify the subcellular localization of ACF7, I used the biochemical fractionation technique. Mouse brains were homogenized and separated into different subcellular compartments. ACF7 was present in both crude cytosolic fraction

(S1) and crude synaptosomal membrane fraction (P2). To reveal the synaptic location of ACF7, I further separated synaptosomal membrane to a synaptic vesicle enriched fraction (SV) and Triton X-100 treated postsynaptic density fractions (PSD-1T and -2T). ACF7 was present in triton-treated PSD fractions but its enrichment was lower than that of PSD-95 (Figure 5C). Furthermore, ACF7 content was relatively low in the SV fraction. These results suggest that ACF7 exists in synaptic sites, but not in synaptic vesicles. To further clarify the localization of ACF7 in hippocampal neurons, double-labeling with synaptic marker proteins was preformed. ACF7 clusters partially overlapped with PSD-95, but its localization was systematically shifted toward to dendritic shafts compared with PSD-95 (Figure 5D). Positions of ACF7 clusters localized were close, but distinct from the presynaptic boutons immunoreactive with synaptophysin antibody (Figure 5E). These results further support that ACF7 localized at postsynaptic sites rather than presynaptic terminals. These immunocytochemical and biochemical analyses suggest that ACF7 is widely distributed throughout neurons, and it accumulates at postsynaptic sites.

Synaptic clusters of ACF7 were independent of microtubules

There are a wide variety of PSD proteins within spines that show heterogeneity in the modes of attachment to the cytoskeleton[57,58]. ACF7 can directly bind to both MT and F-actin,

and it accumulated to the postsynaptic sites (Figures 5B and D). To reveal the molecular mechanisms underlying postsynaptic clustering of ACF7, hippocampal neurons at 3 weeks after plating were treated with the F-actin-depolymerizing agent latrunculin A, or with the MT-depolymerizing agent vincristine. In the control neurons in culture, ACF7 showed synaptic clustering at the region where MTs and F-actin were in close contact (Figure 6A). Treatment with vincristine had no effect on the synaptic clustering of ACF7 which remained colocalized with F-actin. However some ACF7 strongly accumulated on the tubulin paracrystals after treatment with vincristine (Figure 6B). Treatment with latrunculin A caused a dispersal of the synaptic clustering of ACF7 (Figure 6C). These results indicate that synaptic localization of ACF7 in dendritic spines is independent of MT bundles but partly dependent on intact F-actin.

Presence of ACF7 clusters at a subset of dendritic spines

To further clarify the localization of ACF7 in postsynaptic neurons, hippocampal neurons at 7 DIV were transfected with GFP as a volume marker, and fixes at 2 weeks after transfection. Neurons were stained with anti-ACF7 antibody. The ACF7 clusters were present in spines, with preferential localization at the base of spines or in the neck (Figure 7A). Not all dendritic spines were positive with ACF7 clusters (Figure 7A). Thus, I quantified the

proportion of the ACF7 clusters positive spines at 21 DIV. About 15 % of spines contained the synaptic clusters of ACF7 (Figures 7A and B), and these dendritic spines were relatively larger than others (Figure 7C). These data indicate a possible role for ACF7 clusters in dendritic spines.

Overexpression of ACF7 induced local maturation of individual spines containing ACF7 clusters

My data so far indicate a relation between synaptic clusters of ACF7 and regulation of postsynaptic development. To reveal the local effect of ACF7 synaptic clusters, I selected ACF7-GFP as a marker of individual synaptic clusters and evaluated a-gain-of-function phenotype of spines. Hippocampal neurons were transfected with ACF7-GFP together with *lacZ*, and spine morphology was visualized by anti-β-galactosidase immunostaining at 12 days after transfection. The synaptic clustering of ACF7-GFP was observed close to PSD-95 at a subset of dendritic spines (Figure 8A). In neurons overexpressing ACF7-GFP, there was a increase of dendritic protrusion compared with GFP expressing neurons (Figure 8C).

The GFP fluorescence enabled us to divide dendritic spines into two groups; ACF7(-) spines (without accumulation of ACF7-GFP) or ACF7(+) spines (with accumulation of ACF7-GFP). Then, I analyzed the local effect of individual spines with or without ACF7 clusters. Both

spine volume and PSD-95 immunoreactivity were comparable in ACF7(-) spines and GFP transfected neurons. However, ACF7(+) spines were significantly larger (Figure 8D) and also contained more PSD-95 (Figure 8E). These results suggests that ACF7 synaptic clusters contributes to local maturation of individual spines.

ACF7-knockdown suppresses postsynaptic maturation

To further confirm the function of endogenous ACF7 protein in postsynaptic development, I performed loss-of-function analysis in the synaptogenic stage of developing neurons in culture. Hippocampal neurons were transfected with the ACF7 shRNA together with GFP at 9 DIV and dendrite morphology was evaluated at 5 days after transfection. Transfection with ACF7 shRNA at 9 DIV did not result in obvious impairment of dendritic growth. Thus, I focused on spine morphology. Neurons treated with ACF7 shRNA developed less mature dendritic spines, width were thin and with smaller heads (Figure 9A). Density of dendritic protrusions was not changed significantly with or without expression of ACF7 shRNA (Figure 9B). However, dendritic protrusion lengths were increased about ~150 % in ACF7 shRNA transfected neurons (Figure 9C). This phenotypes of ACF7-knockdown were rescued by expression of an RNAi-resistant form of ACF7.

Next, I evaluated spine phenotypes in mature neurons. Hippocampal neurons were transfected with the ACF7 shRNA together with GFP at 9 DIV, and spine morphology was

evaluated at 13 days after transfection. Morphology of spines in neurons expressing ACF7 shRNA was different from control in several aspects (Figure 9D). First, they tended to have small spine heads. Second, the lengths of spines were also increased in mature neurons. Thus, I classified spines into mushroom spines or thin spines using the criteria by spine length and width, and evaluated the fraction of mushroom spines in ACF7 shRNA expressing neurons. The fraction of mushroom-type spines was decreased in neurons expressing ACF7 shRNA (Figure 9E). Furthermore, PSD-95 immunoreactivity was also decreased in ACF7 shRNA expressing neurons (Figure 9F). These results indicates that ACF7 is essential for normal excitatory synapse development.

Discussion

Increasing evidences have suggested that essential roles for the spectraplakin family proteins in the nervous systems[47,55,59–63]. However due to lethality resulting from both complete and nervous tissue specific ACF7 null mutations[46,47,50], the physiological significance of ACF7 in developing neurons has remained unclear. Using hippocampal dissociated culture as a model system and by manipulating ACF7 content at different developmental stages, I provide important insights into roles of ACF7 in mammalian neurons. My study shows that ACF7 is required for both dendrite growth and normal postsynaptic maturation.

Regulation of dendritic growth by ACF7

The importance of spectraplakins in nervous tissue has been identified primarily from the phenotype of *Drosophila shot* mutant, which has defects in terminal branch formation of motor neurons and local sprouting of dendrites[16,17,37,40,55,60,61,63–68]. In the mammalian genome, there are two spectraplakins, ACF7/MACF1 and Bpag1/dystonin. The distribution patterns of ACF7 and Bpag1 are distinct in embryonic day 14.5[69]. ACF7 is prominent in skeletal muscle, lung and the central nervous systems, by contrast, Bpag1 is enriched in skin, heart and the

peripheral nervous system[69,70]. Although ACF7 is shown to be essential for normal brain development including neuronal migration and axonal outgrowth in multiple brain areas[47], the role of mammalian spectraplakins in dendrite morphology is not clear. My biochemical data provide the continuous expression of ACF7 in the postnatal brain (Figure 2). Furthermore, I provide the evidence that ACF7 plays important roles in the enhancement of dendrite growth in hippocampal neurons.

It is widely accepted that MT-actin crosstalk is essential for neurite outgrowth and growth cone motility[7,9–13,15,71,72]. ACF7 localized at the region where MTs and F-actin are in close contact in neurite tips (Figures 3A) and in growth cones (Figure 3B). Furthermore, downregulation of ACF7 suppressed dendritic outgrowth (Figure 4). These results support the idea that spectraplakins directly bind to both MTs and F-actin, and contribute to establish proper neuronal morphology[42,62,65]. In non-neuronal cells, ACF7 accumulates to the tip of growing MTs and coordinates MT dynamics with F-actin in the peripheral region[41,50]. In this study, the localization pattern of ACF7 was similar to +Tips at the peripheral domain in growth cones (Figure 3B). A recent report showed that the +Tip protein EB3 binds directly to the F-actin associated protein drebrin in the growth cone[71]. In this case, MT-actin interaction is mediated by multiple interactions between cytoskeletal associated proteins[15].

ACF7-mediated MT-actin interaction is unique, as it is mediated by a single crosslinking molecule with a huge molecular weight. Thus, I propose that the modes of MT-actin interaction at the tip of MTs is regulated by multiple pathways, and ACF7 has a distinct role in this process. Although there is still much to understand in the molecular mechanisms of MT-actin interaction, my results provide new insights into cytoskeletal crosstalk during neuronal growth.

Regulation of postsynaptic function byACF7

In this study, I provide the evidence that ACF7 is a postsynaptic protein in the mouse brain. It has long been thought that the molecular organization of PSD proteins and cytoskeletons can influence spine shape and contribute to synaptic plasticity[73–75] . Although the PSD proteins are listed by recent proteomic analyses of biochemically purified PSD fractions[48,49], the detailed molecular organization of excitatory synapses is not well understood. The identification of ACF7 as a PSD protein provides new insight into understanding postsynaptic protein network in spines. Although it is still unclear whether ACF7 is a core component of PSD or not, my fluorescent microscopic data showed that ACF7 localization at the base of spines (Figures 5D and 8E).

Even though ACF7 can directly bind to both MTs and F-actin, the synaptic clustering of

ACF7 was diminished after treatment with latrunculin A but not with vincristine (Figure 6). F-actin is a major cytoskeletal component in dendritic spines and plays important roles in anchoring postsynaptic receptors and organizing the PSD[57,58]. Thus, I speculate that the actin binding domain regulates targeting of ACF7 to spines and recruitment of ACF7 to spines initiates its function as a scaffolding protein. There are some evidences that spectraplakins may act as scaffolding proteins to organize the assembly of protein complexes[46,76,77]. Interestingly, the synaptic clustering of ACF7 was detected preferentially at larger spines, and the accumulation was not increased after MT depolymerization. These results suggest that F-actin is not the only mediator of ACF7 synaptic accumulation. ACF7, with its huge molecular size (>600 kDa), contains multiple domains, which may bind to as yet unidentified interacting partner in the PSD.

In this study, I provide evidence for the role of ACF7 in the regulation of postsynaptic functions. Downregulation of ACF7 by siRNA suppressed normal growth of excitatory synapses and moderate overexpression of ACF7 increased spine structural maturation by its clustering in a subset of spines (Figures 8 and 9). The importance of ACF7 function in postsynaptic sites was not predicted from invertebrate studies. I have not yet revealed the clear molecular mechanisms underlying ACF7 dependent postsynaptic growth. However,

accumulating evidences suggests that spectraplakins function as cytoskeletal crosslinkers rather than as independent modulation of MT and F-actin systems in a variety of cell types[17,41,42,50,66].

In non-neuronal cells, ACF7 preferentially accumulates at the tip of MTs, where it coordinates growth of MTs along F-actin when the tips of MTs reach focal adhesions[41]. My immunocytochemical studies provide a molecular model that ACF7 accumulates at a subset of spines, where it regulates the tips of MT penetrating into spines. Detailed localization of ACF7 in spines remain elusive from my light microscopic studies, however this pattern is distinct from CRIPT localization near the post synaptic membrane, which may bind with both MT and PSD-95[78].

If ACF7 also changes the retention time of the dynamic MT plus ends along F-actin in spines, it may contribute to MT-dependent spine enlargement[26,35]. It is also possible that the slowing MT dynamics allows for MT stabilization by other MT binding proteins in spines.. It is known that tubulin and a wide variety of MTs binding proteins are enriched in the PSD fractions, including MAP1b, MAP2, CLASPs, CRIPT, DCLKs and APC[48,49,52,78–80]. In fact, electron microscopic studies of synapses in the brain tissue show the localization of MTs in postsynaptic terminals of larger dendritic spines of some pyramidal neurons[56,81–84]. The MTs in dendritic spines may control organelle positioning and serves as polarized tracks to deliver

synaptic molecules via MT dependent motor proteins[31,32,85].

In this study, I provide a novel role of a mammalian spectraplakin ACF7 in the regulation of synaptic development. I postulate that ACF7 accumulates to the larger spines by F-actin dependent molecular mechanisms and regulate the dynamics of MTs penetrating into dendritic spines. This MT-actin interaction in dendritic spines may act as the basis of postsynaptic molecular networks and maintain proper development of excitatory post synapses.

Acknowledgments

I would like to show my greatest appreciation to Professor Shigeo Okabe for his continuous support and mentorship during the course of my Ph.D studies in the Department of Cellular Neurobiology.

I am also thankful to Dr. Hirohide Iwasaki, Dr. Shinji Tanaka, Dr. Saman Ebrahimi, Masaaki Isshiki, Kazuki Obashi, Reiko Watanabe, Kana Okubo and Takao Nishiguchi for their enormous support and advice, and all the members of Okabe laboratory for their assistance. I would like to thank Japan Society for the Promotion of Science for their financial support.

Finally, I would like to extend my gratitude to my sincere friends for their support. I am sincerely thankful to my parents, brother and my best fellow for their warm encouragement throughout my study.

References

1. Okabe, S. Fluorescence imaging of synapse formation and remodeling. *J. Electron Microsc. (Tokyo).* **62,** 51–62 (2013).

2. Arimura, N. & Kaibuchi, K. Neuronal polarity: from extracellular signals to intracellular mechanisms. *Nat. Rev. Neurosci.* **8,** 194–205 (2007).

3. Luo, L. Actin cytoskeleton regulation in neuronal morphogenesis and structural plasticity. *Annu. Rev. Cell Dev. Biol.* **18,** 601–35 (2002).

4. McAllister, A. K. Dynamic aspects of CNS synapse formation. *Annu. Rev. Neurosci.* **30,** 425–50 (2007).

5. Holtmaat, A. & Svoboda, K. Experience-dependent structural synaptic plasticity in the mammalian brain. *Nat. Rev. Neurosci.* **10,** 647–58 (2009).

6. Caroni, P., Donato, F. & Muller, D. Structural plasticity upon learning: regulation and functions. *Nat. Rev. Neurosci.* **13,** 478–490 (2012).

7. Dent, E. W. *et al.* Filopodia are required for cortical neurite initiation. *Nat. Cell Biol.* **9,** 1347–59 (2007).

8. Flynn, K. C. *et al.* ADF/Cofilin-Mediated Actin Retrograde Flow Directs Neurite Formation in the Developing Brain. *Neuron* **76,** 1091–1107 (2012).

9. Lowery, L. A. & Van Vactor, D. The trip of the tip: understanding the growth cone machinery. *Nat. Rev. Mol. Cell Biol.* **10,** 332–43 (2009).

10. Dent, E. W. & Kalil, K. Axon Branching Requires Interactions between Dynamic Microtubules and Actin Filaments. *J. Neurosci.* **21,** 9757–9769 (2001).

11. Dent, E. W. & Gertler, F. B. Cytoskeletal Dynamics and Transport in Growth Cone Motility and Axon Guidance. *Neuron* **40,** 209–227 (2003).

12. Geraldo, S. & Gordon-Weeks, P. R. Cytoskeletal dynamics in growth-cone steering. *J. Cell Sci.* **122,** 3595–604 (2009).

13. Pak, C. W., Flynn, K. C. & Bamburg, J. R. Actin-binding proteins take the reins in growth cones. *Nat. Rev. Neurosci.* **9,** 136–47 (2008).

14. Vitriol, E. E. A. & Zheng, J. Q. J. Growth cone travel in space and time: the cellular ensemble of cytoskeleton, adhesion, and membrane. *Neuron* **73,** 1068–81 (2012).

15. Rodriguez, O. C. *et al.* Conserved microtubule-actin interactions in cell movement and morphogenesis. *Nat. Cell Biol.* **5,** 599–609 (2003).

16. Sonnenberg, A. & Liem, R. K. H. Plakins in development and disease. *Exp. Cell Res.* **313,** 2189–203 (2007).

17. Suozzi, K. C., Wu, X. & Fuchs, E. Spectraplakins: Master orchestrators of cytoskeletal dynamics. *J. Cell Biol.* **197,** 465–475 (2012).

18. Hering, H. & Sheng, M. Dendritic spines: structure, dynamics and regulation. *Nat. Rev. Neurosci.* **2,** 880–8 (2001).

19. Cingolani, L. A. & Goda, Y. Actin in action: the interplay between the actin cytoskeleton and synaptic efficacy. *Nat. Rev. Neurosci.* **9,** 344–56 (2008).

20. Hotulainen, P. & Hoogenraad, C. C. Actin in dendritic spines: connecting dynamics to function. *J. Cell Biol.* **189,** 619–29 (2010).

21. Kaech, S., Parmar, H., Roelandse, M., Bornmann, C. & Matus, A. Cytoskeletal microdifferentiation: a mechanism for organizing morphological plasticity in dendrites. *Proc. Natl. Acad. Sci. U. S. A.* **98,** 7086–92 (2001).

22. Korobova, F. & Svitkina, T. Molecular architecture of synaptic actin cytoskeleton in hippocampal neurons reveals a mechanism of dendritic spine morphogenesis. *Mol. Biol. Cell* **21,** 165–76 (2010).

23. Hirokawa, N. The arrangement of actin filaments in the postsynaptic cytoplasm of the cerebellar cortex revealed by quick-freeze deep-etch electron microscopy. *Neurosci. Res.* **6,** 269–275 (1989).

24. Hu, X., Viesselmann, C., Nam, S., Merriam, E. & Dent, E. W. Activity-dependent dynamic microtubule invasion of dendritic spines. *J. Neurosci.* **28,** 13094–105 (2008).

25. Gu, J., Firestein, B. L. & Zheng, J. Q. Microtubules in dendritic spine development. *J. Neurosci.* **28,** 12120–4 (2008).

26. Jaworski, J. *et al.* Dynamic microtubules regulate dendritic spine morphology and synaptic plasticity. *Neuron* **61,** 85–100 (2009).

27. Dillon, C. & Goda, Y. The actin cytoskeleton: integrating form and function at the synapse. *Annu. Rev. Neurosci.* **28,** 25–55 (2005).

28. Goda, Y. & Davis, G. W. Mechanisms of synapse assembly and disassembly. *Neuron* **40,** 243–64 (2003).

29. Conde, C. & Cáceres, A. Microtubule assembly, organization and dynamics in axons and dendrites. *Nat. Rev. Neurosci.* **10,** 319–32 (2009).

30. Hirokawa, N., Noda, Y., Tanaka, Y. & Niwa, S. Kinesin superfamily motor proteins and intracellular transport. *Nat. Rev. Mol. Cell Biol.* **10,** 682–96 (2009).

31. Hirokawa, N., Niwa, S. & Tanaka, Y. Molecular motors in neurons: transport mechanisms and roles in brain function, development, and disease. *Neuron* **68,** 610–38 (2010).

32. Verhey, K. J. & Hammond, J. W. Traffic control: regulation of kinesin motors. *Nat. Rev. Mol. Cell Biol.* **10,** 765–77 (2009).

33. Dent, E. W., Merriam, E. B. & Hu, X. The dynamic cytoskeleton: backbone of dendritic spine plasticity. *Curr. Opin. Neurobiol.* (2010). doi:10.1016/j.conb.2010.08.013

34. Merriam, E. B. *et al.* Synaptic Regulation of Microtubule Dynamics in Dendritic Spines by Calcium, F-Actin, and Drebrin. *J. Neurosci.* **33,** 16471–16482 (2013).

35. Merriam, E. B. *et al.* Dynamic microtubules promote synaptic NMDA receptor-dependent spine enlargement. *PLoS One* **6,** e27688 (2011).

36. Hu, X. *et al.* BDNF-induced increase of PSD-95 in dendritic spines requires dynamic microtubule invasions. *J. Neurosci.* **31,** 15597–603 (2011).

37. Jefferson, J. J. J. J., Leung, C. L. C. & Liem, R. K. H. Plakins: goliaths that link cell junctions and the cytoskeleton. *Nat. Rev. Mol. Cell Biol.* **5,** 542–53 (2004).

38. Leung, C. L., Sun, D., Zheng, M., Knowles, D. R. & Liem, R. K. H. Microtubule actin cross-linking factor (MACF): a hybrid of dystonin and dystrophin that can interact with the actin and microtubule cytoskeletons. *J. Cell Biol.* **147,** 1275–86 (1999).

39. Sun, D., Leung, C. & Liem, R. Characterization of the microtubule binding domain of microtubule actin crosslinking factor (MACF): identification of a novel group of microtubule associated proteins. *J. Cell Sci.* **114,** 161–172 (2001).

40. Subramanian, A. *et al.* Shortstop recruits EB1/APC1 and promotes microtubule assembly at the muscle-tendon junction. *Curr. Biol.* **13,** 1086–95 (2003).

41. Wu, X., Kodama, A. & Fuchs, E. ACF7 regulates cytoskeletal-focal adhesion dynamics and migration and has ATPase activity. *Cell* **135,** 137–48 (2008).

42. Applewhite, D. A. *et al.* The spectraplakin Short stop is an actin-microtubule cross-linker that contributes to organization of the microtubule network. *Mol. Biol. Cell* **21,** 1714–24 (2010).

43. Okuda, T. *et al.* Molecular cloning of macrophin, a human homologue of Drosophila kakapo with a close structural similarity to plectin and dystrophin. *Biochem. Biophys. Res. Commun.* **264,** 568–74 (1999).

44. Gong, T. W., Besirli, C. G. & Lomax, M. I. MACF1 gene structure: a hybrid of plectin and dystrophin. *Mamm. Genome* **12,** 852–61 (2001).

45. Bernier, G., Mathieu, M., De Repentigny, Y., Vidal, S. M. & Kothary, R. Cloning and characterization of mouse ACF7, a novel member of the dystonin subfamily of actin binding proteins. *Genomics* **38,** 19–29 (1996).

46. Chen, H.-J. H., Lin, C. C.-S. C.-M. C., Perez-Olle, R., Leung, C. L. & Liem, R. K. H. The role of microtubule actin cross-linking factor 1 (MACF1) in the Wnt signaling pathway. *Genes Dev.* **20,** 1933–45 (2006).

47. Goryunov, D., He, C.-Z., Lin, C.-S., Leung, C. L. & Liem, R. K. H. Nervous-tissue-specific elimination of microtubule-actin crosslinking factor 1a results in multiple developmental defects in the mouse brain. *Mol. Cell. Neurosci.* **44,** 1–14 (2010).

48. Peng, J. *et al.* Semiquantitative proteomic analysis of rat forebrain postsynaptic density fractions by mass spectrometry. *J. Biol. Chem.* **279,** 21003–11 (2004).

49. Chen, X. *et al.* Mass of the postsynaptic density and enumeration of three key molecules. *Proc. Natl. Acad. Sci. U. S. A.* **102,** 11551–6 (2005).

50. Kodama, A., Karakesisoglou, I., Wong, E., Vaezi, A. & Fuchs, E. ACF7 : an essential integrator of microtubule dynamics. *Cell* **115,** 343–354 (2003).

51. Kawabata, I. *et al.* LIS1-dependent retrograde translocation of excitatory synapses in developing interneuron dendrites. *Nat. Commun.* **3,** 722 (2012).

52. Shin, E. *et al.* Doublecortin-like kinase enhances dendritic remodelling and negatively regulates synapse maturation. *Nat. Commun.* **4,** 1440 (2013).

53. Carlin, R. K., Grab, D. J., Cohen, R. S. & Siekevitz, P. Isolation and characterization of postsynaptic densities from various brain regions: enrichment of different types of postsynaptic densities. *J. Cell Biol.* **86,** 831–45 (1980).

54. Cho, K. O., Hunt, C. A. & Kennedy, M. B. The rat brain postsynaptic density fraction contains a homolog of the Drosophila discs-large tumor suppressor protein. *Neuron* **9,** 929–42 (1992).

55. Sanchez-Soriano, N. *et al.* Mouse ACF7 and drosophila short stop modulate filopodia formation and microtubule organisation during neuronal growth. *J. Cell Sci.* **122,** 2534–42 (2009).

56. Westrum, L. E., Jones, D. H., Gray, E. G. & Barron, J. Microtubules, dendritic spines and spine apparatuses. *Cell Tissue Res.* **208,** (1980).

57. Allison, D. W., Chervin, a S., Gelfand, V. I. & Craig, a M. Postsynaptic scaffolds of excitatory and inhibitory synapses in hippocampal neurons: maintenance of core components independent of actin filaments and microtubules. *J. Neurosci.* **20,** 4545–54 (2000).

58. Kuriu, T., Inoue, A., Bito, H., Sobue, K. & Okabe, S. Differential control of postsynaptic density scaffolds via actin-dependent and -independent mechanisms. *J. Neurosci.* **26,** 7693–706 (2006).

59. Röper, K., Gregory, S. L. & Brown, N. H. The “spectraplakins”: cytoskeletal giants with characteristics of both spectrin and plakin families. *J. Cell Sci.* **115,** 4215–25 (2002).

60. Gao, F. B., Brenman, J. E., Jan, L. Y. & Jan, Y. N. Genes regulating dendritic outgrowth, branching, and routing in Drosophila. *Genes Dev.* **13,** 2549–61 (1999).

61. Lee, S., Harris, K. L., Whitington, P. M. & Kolodziej, P. A. short stop is allelic to kakapo, and encodes rod-like cytoskeletal-associated proteins required for axon extension. *J. Neurosci.* **20,** 1096–108 (2000).

62. Lee, S. & Kolodziej, P. A. Short Stop provides an essential link between F-actin and microtubules during axon extension. *Development* **129,** 1195–204 (2002).

63. Lee, S. *et al.* The F-actin-microtubule crosslinker Shot is a platform for Krasavietz-mediated translational regulation of midline axon repulsion. *Development* **134,** 1767–77 (2007).

64. Applewhite, D. A., Grode, K. D., Duncan, M. C. & Rogers, S. L. The actin-microtubule cross-linking activity of Drosophila Short stop is regulated by intramolecular inhibition. *Mol. Biol. Cell* **24,** 2885–93 (2013).

65. Alves-Silva, J. *et al.* Spectraplakins Promote Microtubule-Mediated Axonal Growth by Functioning As Structural Microtubule-Associated Proteins and EB1-Dependent +TIPs (Tip Interacting Proteins). *J. Neurosci.* **32,** 9143–58 (2012).

66. Bottenberg, W. *et al.* Context-specific requirements of functional domains of the Spectraplakin Short stop in vivo. *Mech. Dev.* **126,** 489–502 (2009).

67. Strumpf, D. Kakapo, a Novel Cytoskeletal-associated Protein Is Essential for the Restricted Localization of the Neuregulin-like Factor, Vein, at the Muscle-Tendon Junction Site. *J. Cell Biol.* **143,** 1259–1270 (1998).

68. Gregory, S. L. & Brown, N. H. kakapo, a gene required for adhesion between and within cell layers in Drosophila, encodes a large cytoskeletal linker protein related to plectin and dystrophin. *J. Cell Biol.* **143,** 1271–82 (1998).

69. Leung, C. L., Zheng, M., Prater, S. M. & Liem, R. K. H. The BPAG1 locus: Alternative splicing produces multiple isoforms with distinct cytoskeletal linker

domains, including predominant isoforms in neurons and muscles. *J. Cell Biol.* **154,** 691–7 (2001).

70. Bernier, G. *et al.* Acf7 (MACF) is an actin and microtubule linker protein whose expression predominates in neural, muscle, and lung development. *Dev. Dyn.* **219,** 216–25 (2000).

71. Geraldo, S., Khanzada, U. K., Parsons, M., Chilton, J. K. & Gordon-Weeks, P. R. Targeting of the F-actin-binding protein drebrin by the microtubule plus-tip protein EB3 is required for neuritogenesis. *Nat. Cell Biol.* **10,** 1181–9 (2008).

72. Dent, E. W., Callaway, J. L., Szebenyi, G., Baas, P. W. & Kalil, K. Reorganization and Movement of Microtubules in Axonal Growth Cones and Developing Interstitial Branches. *J. Neurosci.* **19,** 8894–8908 (1999).

73. Sheng, M. & Hoogenraad, C. C. The postsynaptic architecture of excitatory synapses: a more quantitative view. *Annu. Rev. Biochem.* **76,** 823–47 (2007).

74. Okabe, S. Molecular anatomy of the postsynaptic density. *Mol. Cell. Neurosci.* **34,** 503–18 (2007).

75. Feng, W. & Zhang, M. Organization and dynamics of PDZ-domain-related supramodules in the postsynaptic density. *Nat. Rev. Neurosci.* **10,** 87–99 (2009).

76. Strumpf, D. & Volk, T. Kakapo, a novel cytoskeletal-associated protein is essential for the restricted localization of the neuregulin-like factor, vein, at the muscle-tendon junction site. *J. Cell Biol.* **143,** 1259–70 (1998).

77. Antolik, C. *et al.* The actin binding domain of ACF7 binds directly to the tetratricopeptide repeat domains of rapsyn. *Neuroscience* **145,** 56–65 (2007).

78. Valtschanoff, J. G. & Weinberg, R. J. Laminar organization of the NMDA receptor complex within the postsynaptic density. *J. Neurosci.* **21,** 1211–7 (2001).

79. Niethammer, M. *et al.* CRIPT, a novel postsynaptic protein that binds to the third PDZ domain of PSD-95/SAP90. *Neuron* **20,** 693–707 (1998).

80. Passafaro, M., Sala, C., Niethammer, M. & Sheng, M. Microtubule binding by CRIPT and its potential role in the synaptic clustering of PSD-95. *Nat. Neurosci.* **2,** 1063–9 (1999).

81. Gray, E. G., Westrum, L. E., Burgoyne, R. D. & Barron, J. Synaptic organisation and neuron microtubule distribution. *Cell Tissue Res.* **226,** (1982).

82. Westrum, L. E., Gray, E. G., Burgoyne, R. D. & Barron, J. Synaptic development and microtubule organization. *Cell Tissue Res.* **231,** (1983).

83. Fiala, J. C. *et al.* Timing of neuronal and glial ultrastructure disruption during brain slice preparation and recovery in vitro. *J. Comp. Neurol.* **465,** 90–103 (2003).

84. Chicurel, M. E. & Harris, K. M. Three-dimensional analysis of the structure and composition of CA3 branched dendritic spines and their synaptic relationships with mossy fiber boutons in the rat hippocampus. *J. Comp. Neurol.* **325,** 169–82 (1992).

85. Hirokawa, N., Nitta, R. & Okada, Y. The mechanisms of kinesin motor motility: lessons from the monomeric motor KIF1A. *Nat. Rev. Mol. Cell Biol.* **10,** 877–84 (2009).

Figure legends

Figure 1. Domain organization of ACF7/MACF1

(A) ACF7/MACF1 is composed of seven domains: CH1 and CH2 domains, a plakin domain, an α-helical spectrin repeat domain, two EF hands, a GAR domain and a CTD domain. CH domains directly bind to F-actin. Some isoforms of ACF7 which lack the CH1 domain have weaker binding to F-actin. The GAR domain binds to and stabilizes MTs. CTD domain interact with EB1/3; proteins which bind to the growing ends of MTs.

(B) A working model of ACF7 in MT-actin coordination in non-neuronal cell. The CTD domain interacts with EB1/3, and ACF7 localizes at the tip of MTs similar to other plus end tracking proteins (Ⅰ). When the tip of MTs arrive at actin rich regions, ACF7 interacts with F-actin (Ⅱ). ACF7 strongly associates with the lateral walls of MTs via its GAR domain, and coordinates dynamics between these two types of cytoskeletal polymers (Ⅲ).

Figure 2. Expression profile of ACF7 protein in the postnatal developmental brain

(A and B) Western blotting analysis of ACF7. Brain tissue extracts were centrifuged to remove the nuclear fraction and resolved by electrophoresis through 6% SDS–polyacrylamide gels. Western blotting analysis were performed with anti-ACF7 antibody against a plakin

domain epitope. The immunoreactive bands of about 600 kDa size corresponding to the size of the full-length ACF7 were detected, (A) in the extracts prepared from multiple brain regions or (B) dissociated hippocampal neurons at various days after plating.

(C) Western blotting of ACF7 knockout cells. MEFs derived from ACF7$^{flox/flox}$ embryos were infected with adenovirus to express Cre recombinase. The immunoreactivity was undetectable 3 days after infection.

Figure 3. Presence of ACF7 in growth cones of immature hippocampal neurons

(A and B) Immunocytochemistry of immature dissociated hippocampal neurons in relation to ACF7 between MTs and F-actin. Neurons at 5 DIV were subjected to tripleimmunofluorescence with anti-ACF7, rhodamine-conjugated phalloidin and anti-α-tubulin antibodies. (A) ACF7 were accumulated at the interphase between MT and F-actin in growth cones at 5 DIV (arrows). (B) ACF7 localized at the transition zone between the central and peripheral domains in growth cones ACF7 accumulated at the interphase between MTs and F-actin (red arrow). ACF7 also showed +Tips-like pattern at the peripheral domain in growth cones (white arrow).

(C) Hippocampal neurons were transfected with ACF7-GFP. The neurons were immunostained with rhodamine-conjugated phalloidin and anti-α-tubulin antibodies at 5 DIV.

ACF7-GFP co-localized with both MT and F-actin (arrow)

Bars; 5 μm for A, 10 μm for B and C

Figure 4. ACF7 is essential for enhancement of dendritic growth

(A-C) Neurons expressing ACF7 shRNA showed severe impairment of dendritic branching (arrows), which could be rescued by expression of shRNA-resistant constructs for ACF7. The shRNA plasmids were transfected to hippocampal neurons at 4 DIV together with GFP and the neuronal morphology were evaluated at 5 days after transfection.

(B and C) Quantification of dendrite morphology in neurons transfected with control or ACF7 shRNA, with or without rescue constructs. Sholl analyses measuring each the number of dendrites intersections at each 20 μm radial segment from the cell soma (B). ACF7 shRNA plasmid expressing neurons caused a decrease (about ~60 %) in the total length of dendrites compared with control shRNA plasmid expressing neurons (C).

(D-E) Neurons expressing ACF7-GFP showed enhancement of dendritic growth, but not its truncated mutants. Hippocampal neurons at 4 DIV were transfected with a various GFP-tagged ACF7 mutants together with *lacZ*. The dendrite morphology was visualized by anti-β-galactosidase immunostaining at 9 DIV. In control samples, GFP expression plasmids were used.

(E and F) Quantification of dendrite morphology in neurons transfected with expression vectors of GFP-tagged a various truncated mutants of ACF7. Sholl analyses of dendritic complexity (E) and evaluation of total dendritic length (F) in the neurons.

(n = each 10 cells, one-way ANOVA followed by Tukey–Kramer multiple comparison tests: *$p < 0.05$, **$p < 0.01$)

Bar; 100 μm for A and D

Figure 5. Presence of ACF7 in postsynaptic compartments

(A) Immunocytochemistry of mature dissociated hippocampal neurons in relation to ACF7 between MTs and F-actin. Neurons at 21 DIV were subjected to tripleimmunofluorescence with anti-ACF7, rhodamine-conjugated phalloidin and anti-α-tubulin antibodies. ACF7 were distributed throughout neurons and accumulated at cell soma in this stage. ACF7 exhibited two different patterns : a MT like staining pattern along dendrite (white arrow) and a cluster staining pattern co-localized with F-actin (red arrow).

(B and C) Double-labeling with synaptic marker proteins. Strong ACF7 clusters co-localized with a subset of PSD-95(B). ACF7 localized at adjacent area of synaptophysin puncta (C).

(D) Presence of ACF7 immunoreactivity in PSD-1T and PSD-2T fractions. Adult mouse brain were homogenized and separated into different subcellular compartments (P2: Crude

synaptosomal pellet, S3: Crude synaptic vesicle fraction,P3: Lysed synaptosomal membrane fraction, SV: Synaptic vesicle fraction, SPM: Synaptic plasma membrane fraction, PSD1T, PSD2T: purified PSD fractions) The isolated subcellular compartments were analyzed by western blotting.

Bars; 50 μm for A, 10 μm for B, D and E

Figure 6. Synaptic clusters of ACF7 was independent of microtubules

(A-C) ACF7 localization after treatment with the F-actin-depolymerizing agent or with the MT-depolymerizing agent. Hippocampal neurons at 3 weeks after plating were treated with latrunculin A or with vincristine and stained with anti-ACF7, rhodamine conjugated phalloidin and anti-α-tubulin antibodies.

(A) In the control neurons, F-actin and MTs seems to be spatially separated. ACF7 showed the synaptic clustering pattern at the region where MTs and F-actin were closely contacted.

(B) Treatment with MT depolymerizing agent vincristine eliminated the MT bundles but unaffected to F-actin within spines. ACF7 synaptic clusters remained with F-actin, and other populations of ACF7 co-localized with tubulin paracrystals after treatment with vincristine.

(C) Treatment with latrunculin A eliminates the F-actin within the neurons, while not affecting MTs. ACF7 clusters were dispersed after treatment with latrunculin A.

Bars; 10 μm for A, B and C

Figure 7. Presence of ACF7 clusters at a subset of dendritic spines

(A- C) Spine localization of ACF7 in GFP transfected neurons. Hippocampal neurons at 7 DIV were transfected with GFP as a volume marker and stained with anti-ACF7 antibody at 21 DIV. The synaptic clustering of ACF7 was presented within spine cytoplasm, and their localization was relatively close to spine neck (A).

(B) Quantification of the proportion of the ACF7 clusters positive spines.

(C) Quantification of spine volume based on GFP fluorescence.

(ACF7(-) spines: n= 4 cells, 178 spines, ACF7(+) spines: n= 4 cells, 24 spines, t-tests: *p < 0.05)

Bar; 10 μm for A

Figure 8. Overexpression of ACF7 induced local maturation of individual spines containing ACF7 clusters

(A) The synaptic clustering of ACF7-GFP were adjacent to PSD-95 within dendritic spines. Hippocampal neurons were transfected ACF7-GFP together with the *lacZ*. At 12 days after transfection, the neurons were stained with anti-PSD-95 and anti-β-galactosidase to visualize

spine morphology.

(B-E) Neurons expressing ACF7-GFP showed enhancement of postsynaptic maturation. Hippocampal neurons at 9 DIV were transfected GFP-tagged protein together with *lacZ*. Spine morphology was visualized by anti-β-galactosidase immunostaining. Spines were divided into two groups; ACF7- spines or ACF7+ spines (with or without accumulation of ACF7-GFP). Dendritic protrusion density (C), spine volume (D) and relative intensity of PSD-95 puncta (E) in neurons expressing GFP and ACF7-GFP (GFP: n =13 cells, ACF-GFP: n = 12 cells, one-way ANOVA followed by Tukey–Kramer multiple comparison tests: **p < 0.01, ***p < 0.001)

Bars; 1 μm for A, 5 μm for B.

Figure 9. ACF7-knockdown suppresses postsynaptic maturation

(A-C) Neurons expressing ACF7 shRNA showed longer dendritic spines (arrows), which could be rescued by expression of shRNA-resistant constructs for ACF7. Hippocampal neurons were transfected with the ACF7 shRNA together with GFP at 9 DIV and spine morphology based on GFP fluorescence were subjected at 14 DIV. Dendritic protrusion length (B) and dendritic protrusion density (C) in neurons transfected with control or ACF7 shRNA, with or without rescue constructs.

(control shRNA: n = 11 cells, ACF7 shRNA: n =10 cells, ACF7 shRNA plus ACF7: n = 11

cells , one-way ANOVA followed by Tukey–Kramer multiple comparison tests:, ***p < 0.001)

(D-F) Reduction of PSD-95 immunoreactivity was observed in ACF7 shRNA expressing neurons. Hippocampal neurons were transfected with the ACF7 shRNA together with GFP at 9 DIV and stained with anti-PSD-95 at 21 DIV. Fractions of mushroom type spines (E) and relative PSD-95 intensity (E) in neurons expressing control shRNA or ACF7 shRNA. (control shRNA: n = 12 cells, ACF7 shRNA: n =12 cells, t-tests: *p < 0.05, ***p < 0.001) Bars; 10 μm for A and D.

Figure 1. Domain organization of ACF7/MACF1

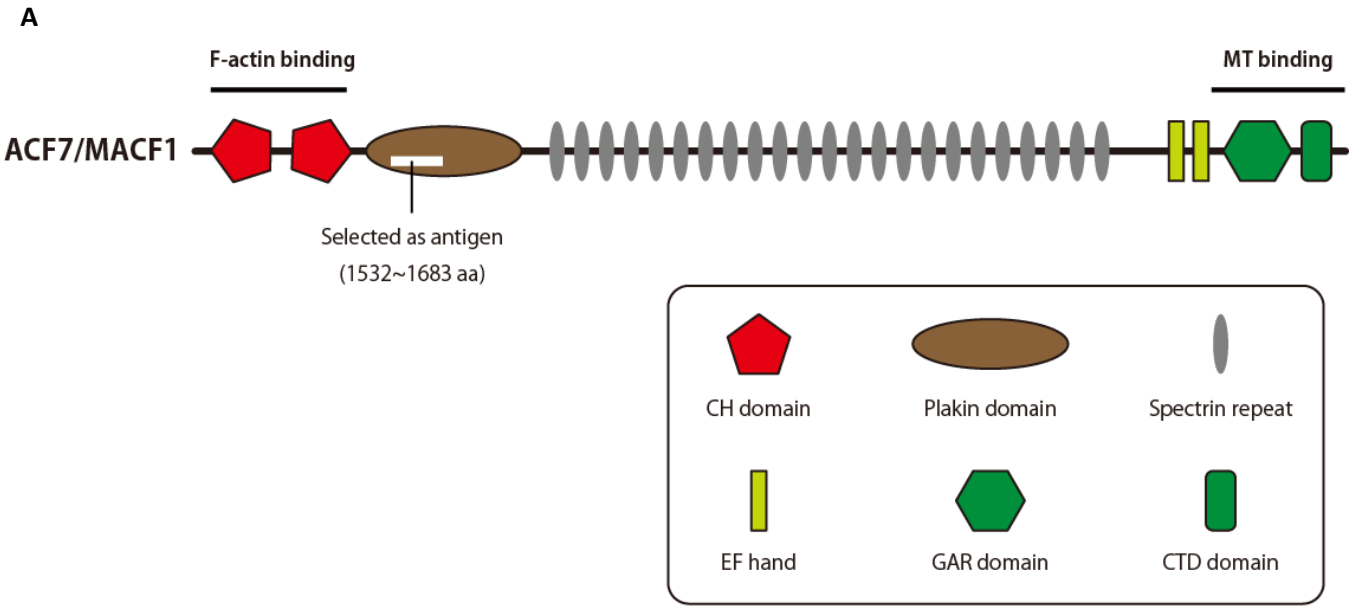

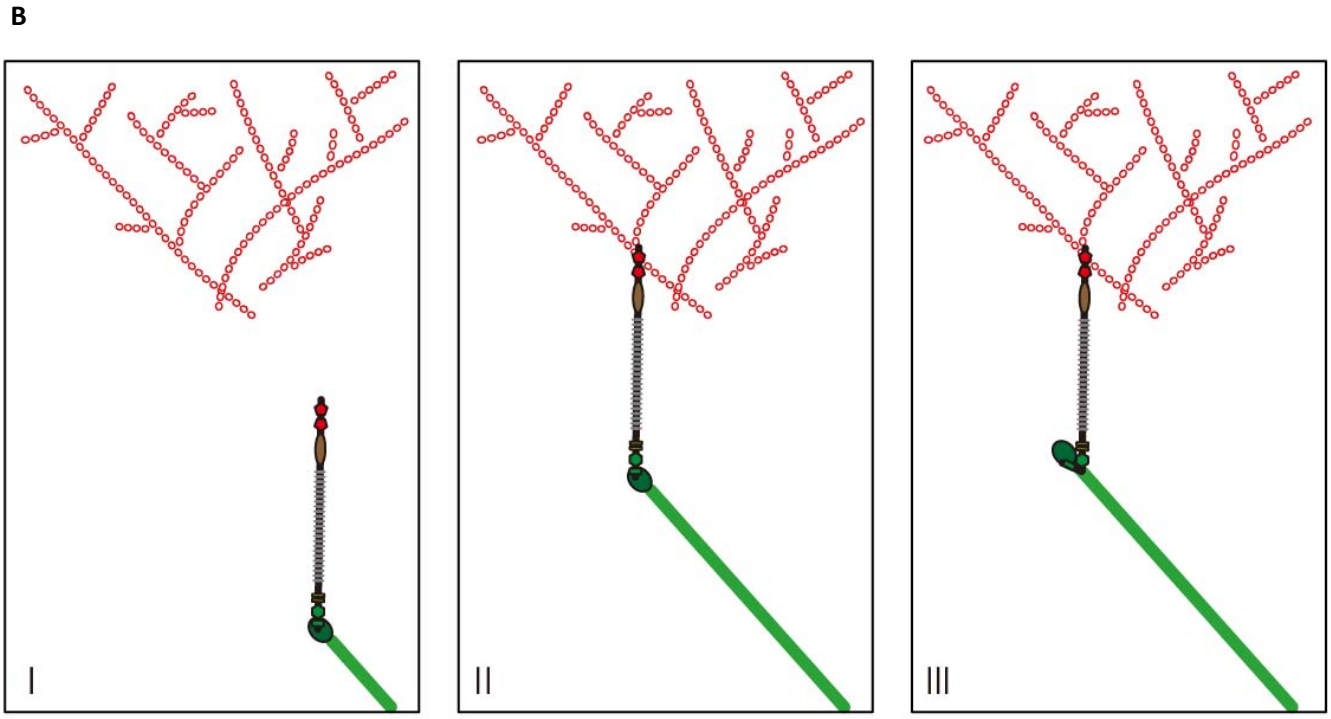

Figure 2. Expression profile of ACF7 protein in the postnatal developing brain

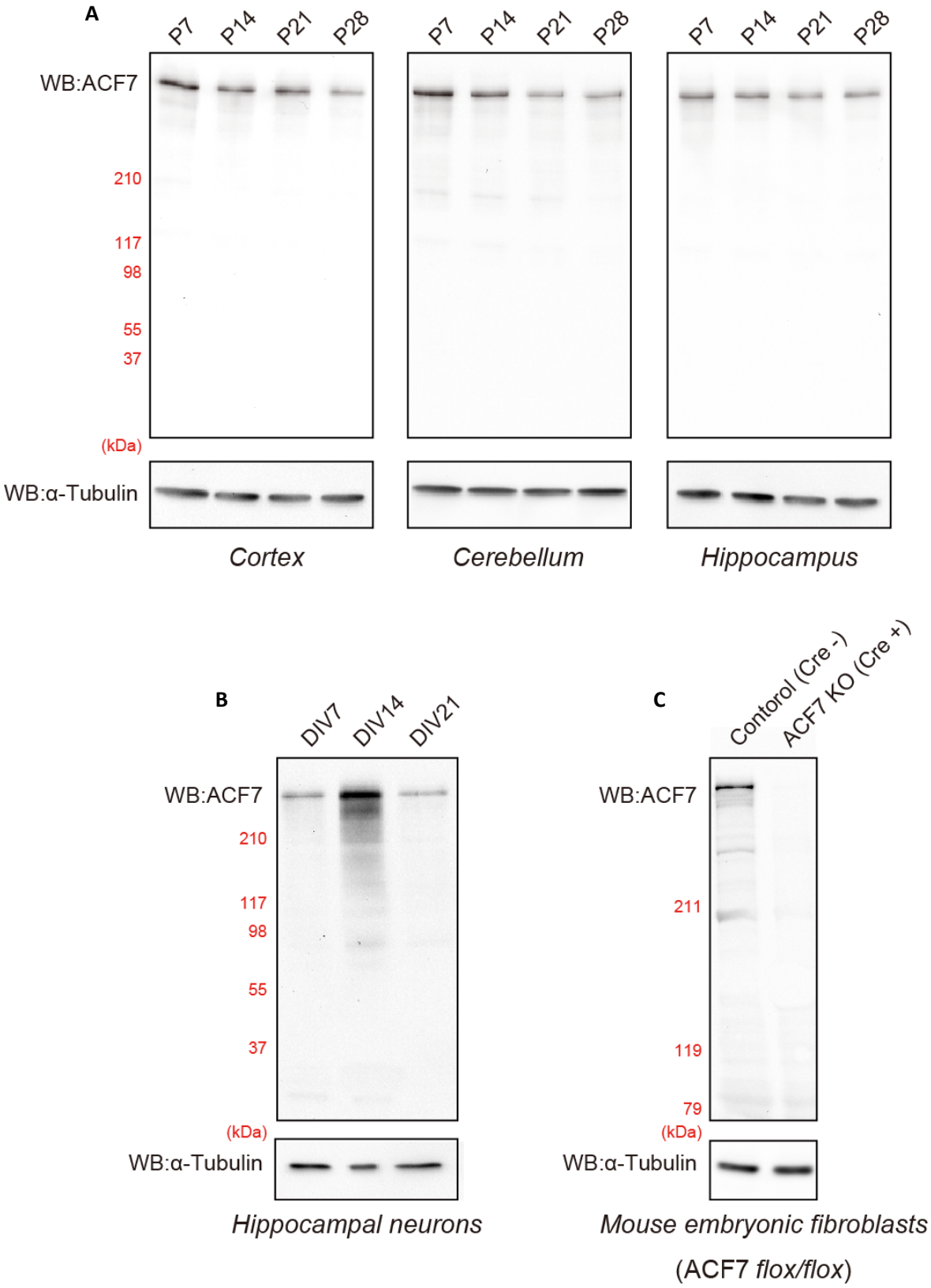

Figure 3. Presence of ACF7 in growth cones of immature hippocampal neurons

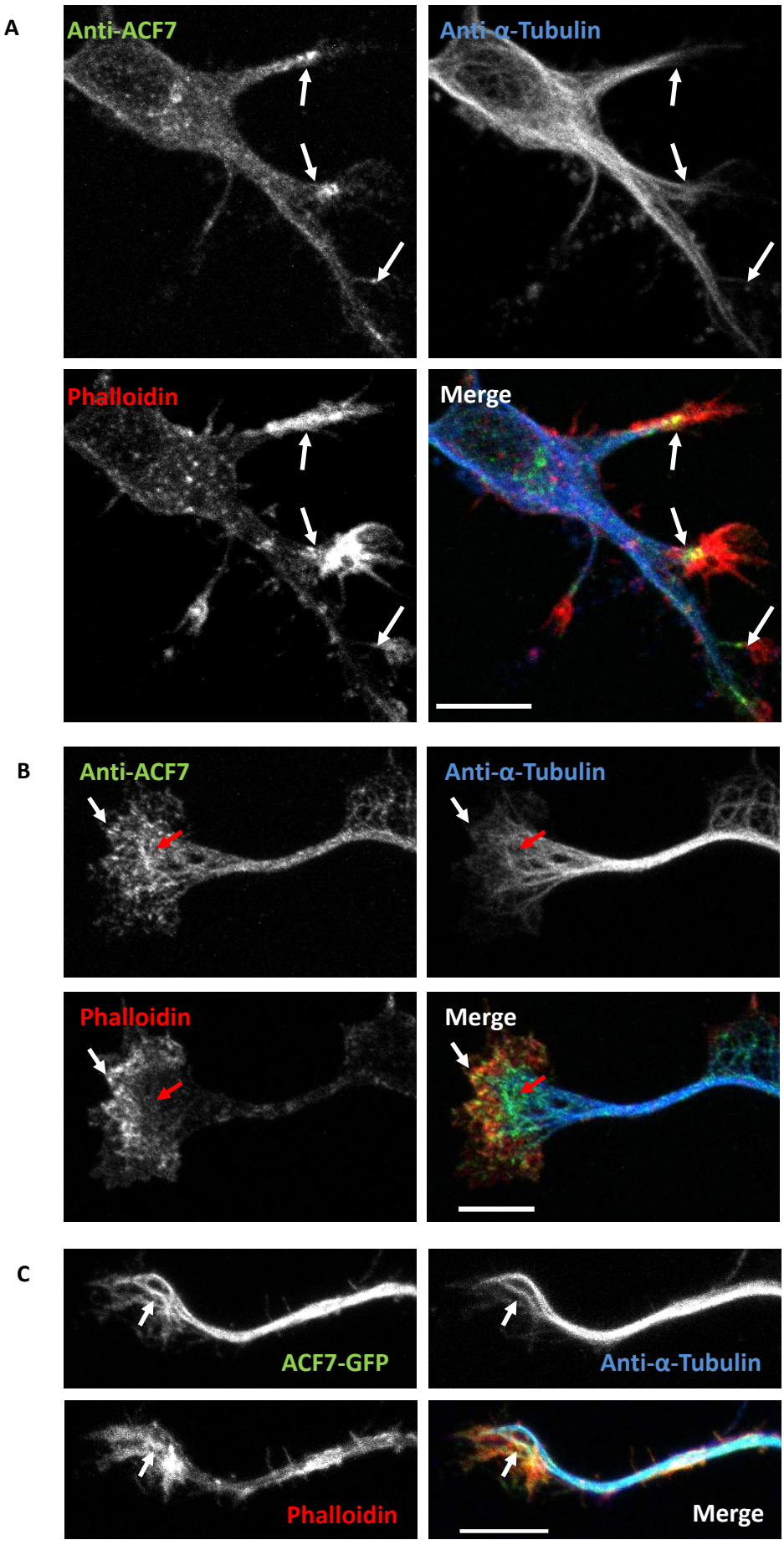

Figure 4. ACF7 is essential for enhancement of dendritic growth

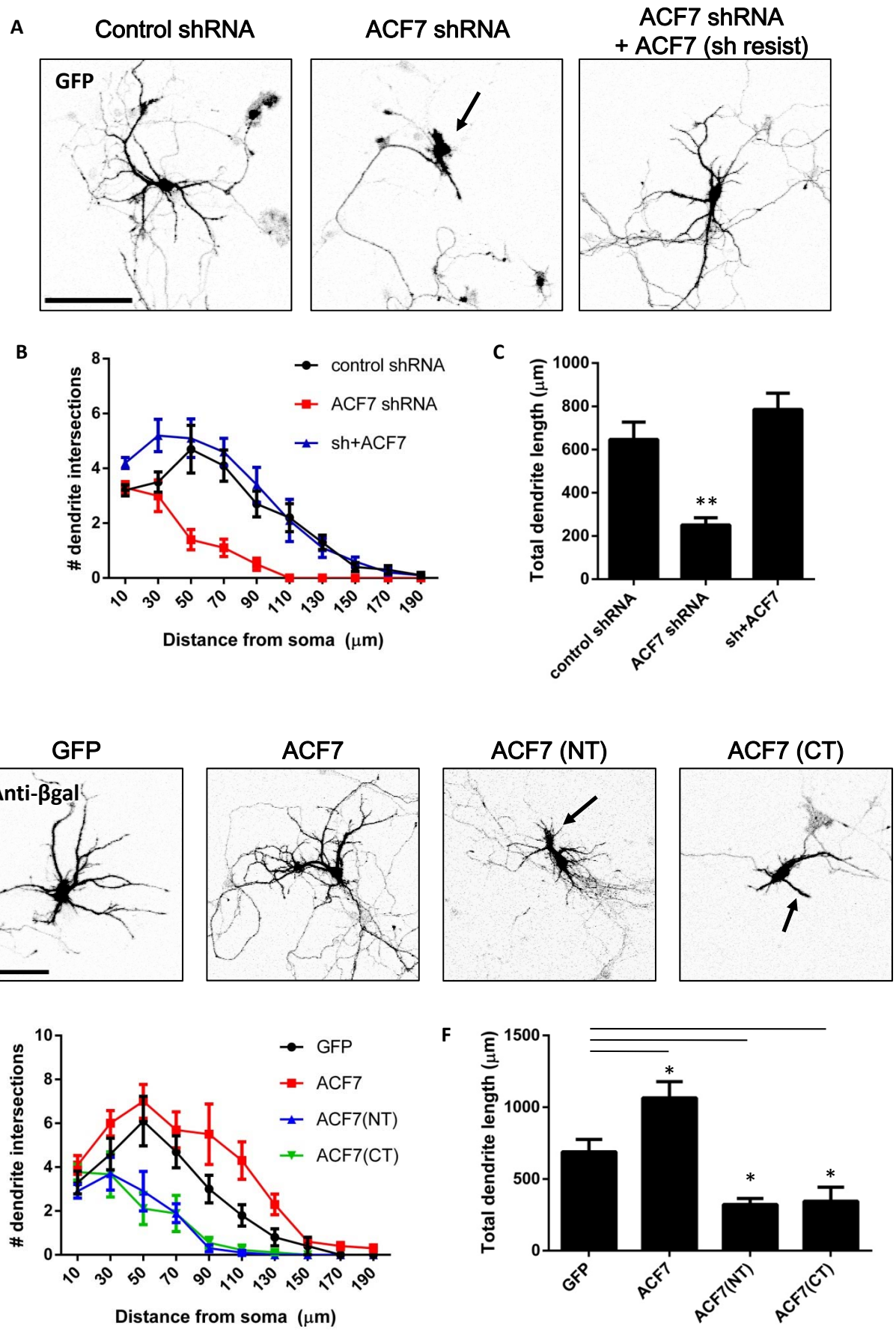

Figure 5. Presence of ACF7 in postsynaptic compartments

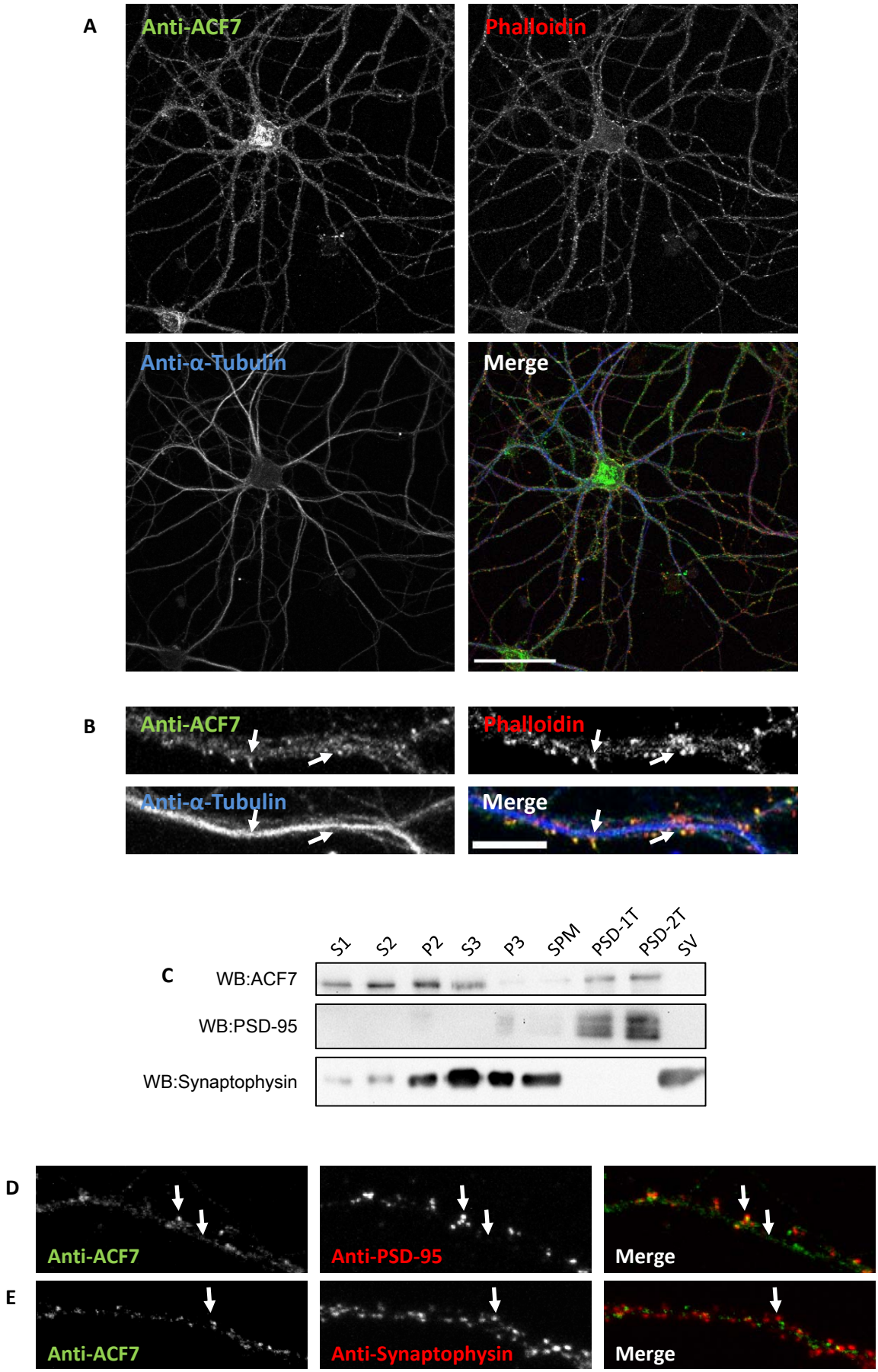

Figure 6. Synaptic clusters of ACF7 was independent of microtubules

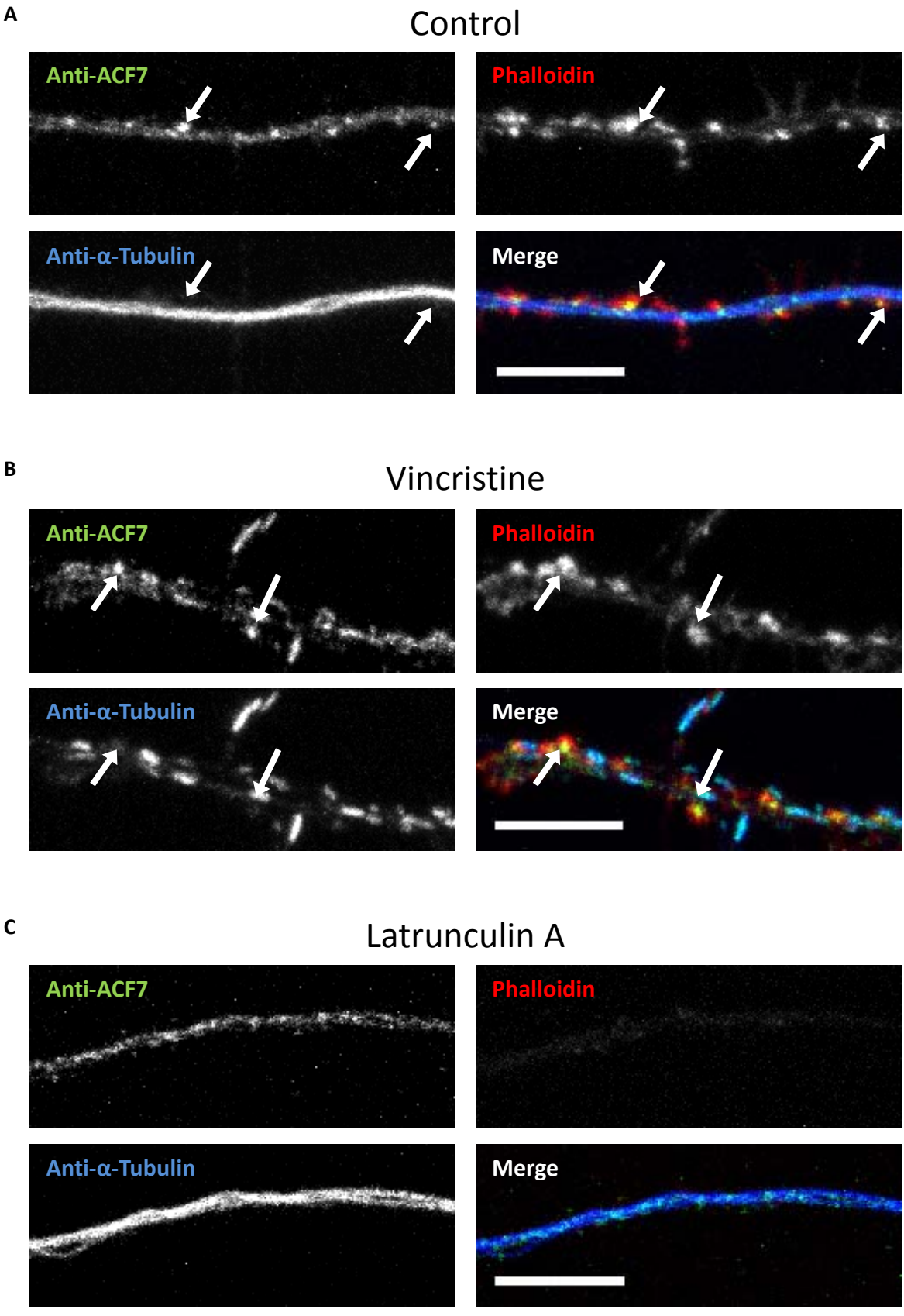

Figure 7. Presence of ACF7 clusters at a subset of dendritic spines

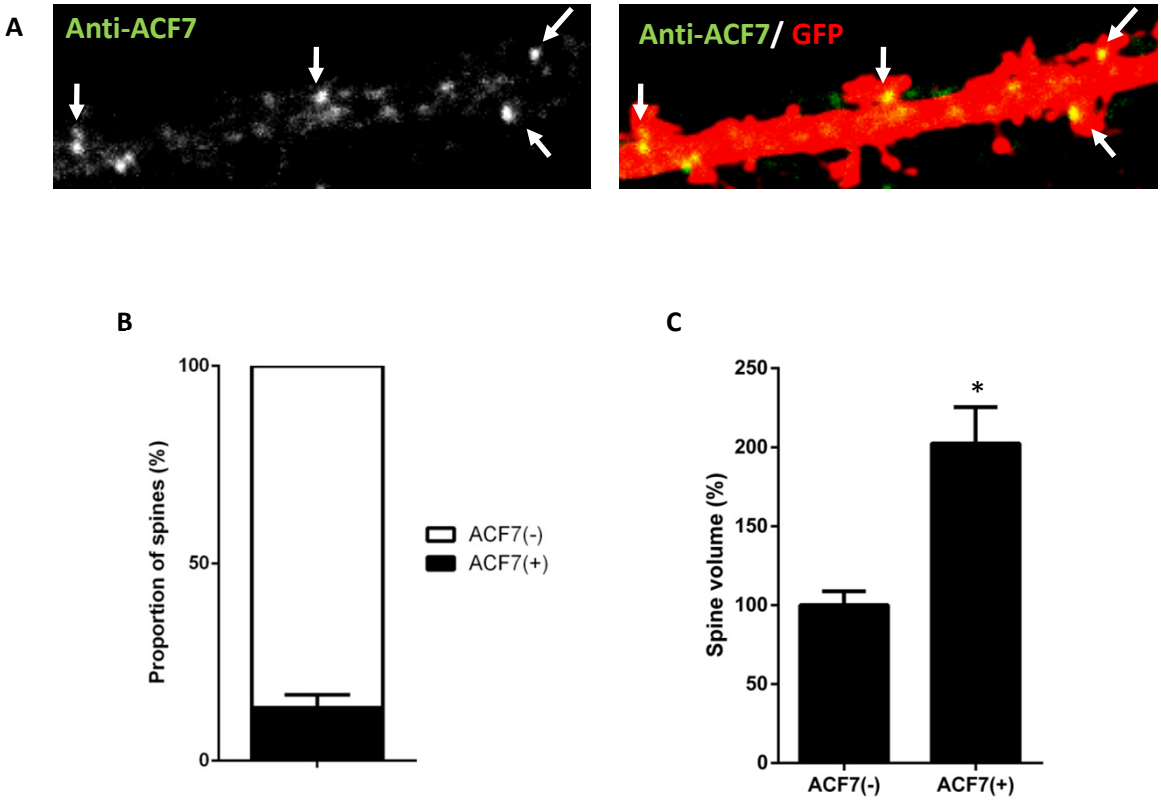

Figure 8. Overexpression of ACF7 induced local maturation of individual spines containing ACF7 clusters

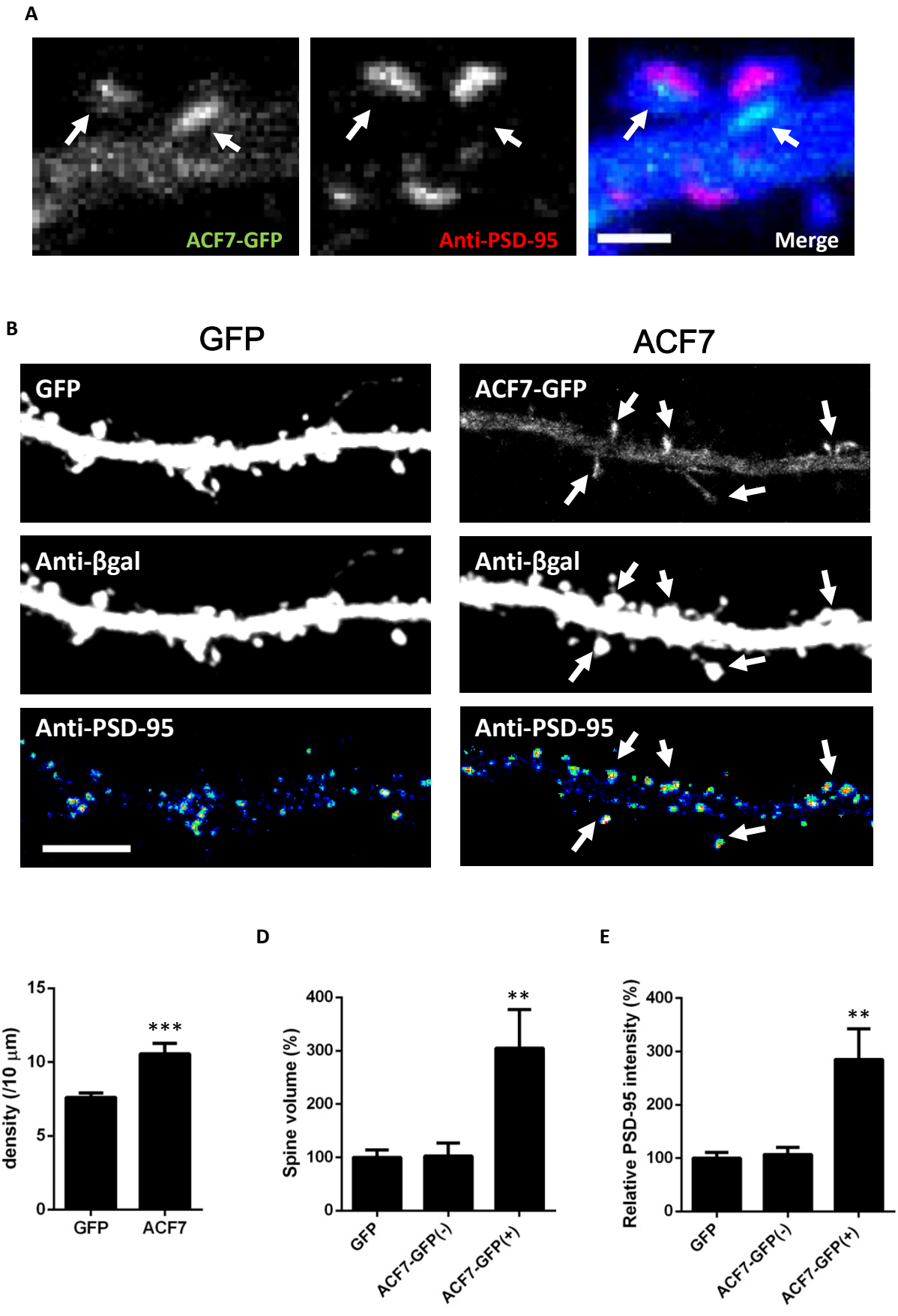

Figure 9. ACF7-knockdown suppresses postsynaptic maturation